RevoMaker: Enabling Multi-directional and Functionally-embedded 3D Printing using a Rotational Cuboidal Platform

Wei Gao[*], **Yunbo Zhang**[*], **Diogo C. Nazzetta, Karthik Ramani, Raymond J. Cipra**
School of Mechanical Engineering, Purdue University
West Lafayette, IN 47907
{gao51, ybzhang, dn, ramani, cipra}@purdue.edu

ABSTRACT

In recent years, 3D printing has gained significant attention from the maker community, academia, and industry to support low-cost and iterative prototyping of designs. Current unidirectional extrusion systems require printing sacrificial material to support printed features such as overhangs. Furthermore, integrating functions such as sensing and actuation into these parts requires additional steps and processes to create "functional enclosures", since design functionality cannot be easily embedded into prototype printing. All of these factors result in relatively high design iteration times.

We present "RevoMaker", a self-contained 3D printer that creates direct out-of-the-printer functional prototypes, using less build material and with substantially less reliance on support structures. By modifying a standard low-cost FDM printer with a revolving cuboidal platform and printing partitioned geometries around cuboidal facets, we achieve a multidirectional additive prototyping process to reduce the print and support material use. Our optimization framework considers various orientations and sizes for the cuboidal base. The mechanical, electronic, and sensory components are preassembled on the flattened laser-cut facets and enclosed inside the cuboid when closed. We demonstrate RevoMaker directly printing a variety of customized and fully-functional product prototypes, such as computer mice and toys, thus illustrating the new affordances of 3D printing for functional product design.

Author Keywords

Multi-directional 3D printing; functional product design.

ACM Classification Keywords

H.5.2 [Information Interfaces and Presentation] : User Interfaces.

---

[*]Wei Gao and Yunbo Zhang contributed equally to this paper
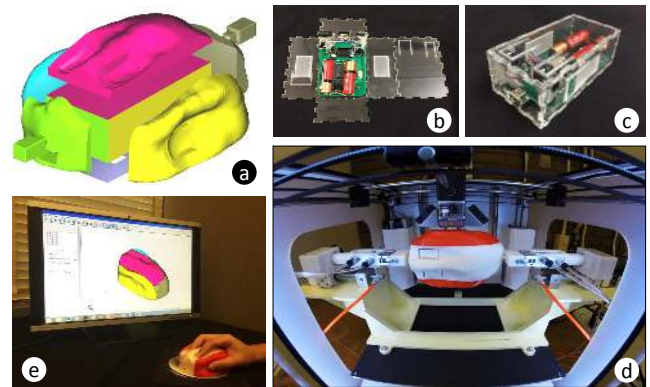
Figure 1. By revolving a laser-cut cuboidal box where functional components are already pre-enclosed inside (b, c), RevoMaker prints partitioned geometries (a) around the cuboid (d) to create a customizable computer mouse (e). We demonstrate a multi-directional and functionally-embedded additive prototyping process to reduce the print and support consumption.

INTRODUCTION

Modern 3D printing techniques have their foundations in four key patents: vat photopolymerization, powder bed fusion, material extrusion, and binder jetting [14, 8, 7, 22]. Among these, the inexpensive and flexible extrusion systems are gaining an extensive popularity among the DIY crowds. The method, popularly referred to as *Fused Deposition Modeling (FDM)*, generates layers by mechanically extruding molten thermoplastic material (e.g., ABS or PLA) onto a substrate.
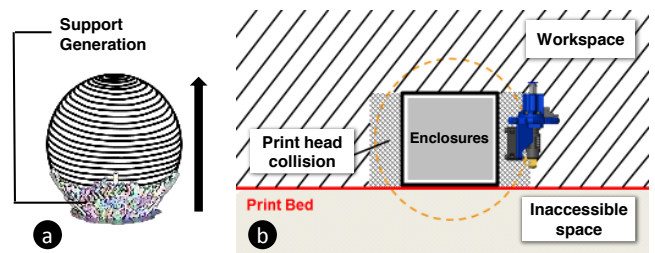

Figure 2. For instance, in order to print a sphere, traditional material extrusion process (a) generates sacrificial material to support printed overhanging features, and (b) has limited reachability if one intends to print around an enclosure
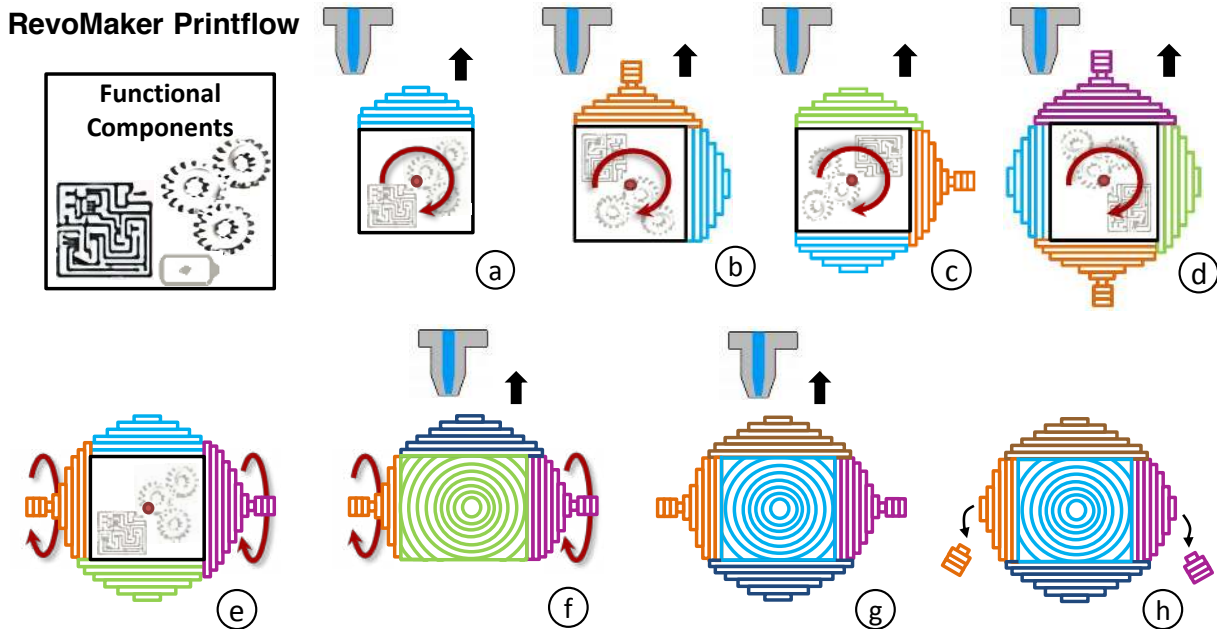
RevoMaker Printflow

Figure 3. (a)-(d) revolving a cuboidal base about the out-of-plane central axis and printing four partitioned geometries around the base. A pair of handles are added to the opposite facets, allowing the cuboid to be gripped for the next run of rotation, (e)-(g) revolving the cuboid about the in-plane central axis and printing the remaining two partitioned geometries, and (h) snapping off two extra handles when the print is completed.

In order to create complex geometries such as overhangs and undercuts, current additive manufacturing systems need to provide means to support the printed features of subsequent layers. In the material extrusion process, this is typically done by printing fine scaffold structures from the build material (See Fig.2(a)). Such sacrificial support structures require additional material and consume a large portion of the printing time. Post-processing operations thereby are necessitated for separating the printed objects with built-in support. The methods and ease of removal of support structure varies by extrusion methods and build materials, including lye bathing for the soluble support, and mechanical cutting and peeling away for the non-soluble support.

In addition, current plastics-based 3D printing is more suitable for fabricating decorative models, design concept prototypes and customized products. Traditional design tools and fabrication methods implicitly prevent designers from encapsulating full functionalities in the early design concept prototyping stage. Therefore, designers are forced to design individual parts using 3D printing, assemble them as done in conventional manufacturing, and iteratively create additional functionalities. We present an alternative 3D printing process that can combine functional design along with the shape creation by embedding components during 3D printing. Unfortunately, using traditional printing and placing such enclosures on the print bed will not allow layer-wise fabrication since the printhead intersects with the enclosure and any geometry beneath the enclosure is infeasible to print (See Fig.2(b)).

We demonstrate a multi-directional 3D printing process that is capable of inherently reducing build and support consumption, and producing a new genre of custom products with higher levels of functionality. The key idea is to enclose functional components inside a laser-cut cuboidal enclosure, which is also a printing base inscribed within a desired shape. By revolving the cuboid shown in Fig.3, we print partitioned geometries on and around each facet. In RevoMaker, the cuboidal base (a) encapsulates advanced functionality the user does not need to have detailed knowledge of, (b) saves time and print material for 3D printing by using laser cutting, (c) doubles up as a platform for 3D printing, and (d) also structurally adheres to the 3D printed material. Our system affords a high manufacturing precision by (a) seamlessly printing exterior skin geometries in a single build (no gap between partitions), (b) enabling directly side-surface functionalities that also interact with housed modules in a compact volume, and (c) ensuring a strong bond within overlapping partitions since the print material fuses with itself. Thus we enlarge the design space of 3D printing to go beyond simple parts using the volume within the 3D printed shape itself to embed functionality. Different use cases that demonstrate the feasibility are discussed later in this paper.

In general, our design goals for RevoMaker are:

- Lesser use of build material

- Significant reduction of support consumption

- Reduced need of post-processing operation

- Embedding of functional components

Currently our approach is more suitable for the object shapes that approximate the cuboid, and requires combining laser cutting process and manual user involvement.

RELATED WORK

Hollowing and optimizing support generation

Previous research studies have been dedicated to reduce both the printing volume and support generation. A natural way to reduce printing volume is to hollow the model based on physical-geometric optimization [28]. Another research intended to improve the structural integrity by generating *honeycomb-cells* inside the model [16]. However, none of these existing methods generate an interior space that is well-structured and fully used for functional enclosures. On the other hand, methods were proposed to reduce support materials by optimizing the model orientation for printing [2, 25], and optimizing support scaffolding structures that consume less material [27, 9, 23, 12]. Due to the unidirectional printing process, the reduction of support in general is quite limited and can hardly be post-processing free.

Fast fabrication of 3D objects

By introducing intermediate low-fidelity fabrication into traditional slow but hi-fidelity printing process, Mueller et al. and Beyer et al. proposed a variety of alternative fabrication methods, such as printing wireframe mesh of an object [18], substituting sub-volumes of a model with standard Lego building blocks [19] and laser-cut parts [4]. These different approaches effectively reduced the printing time while preserving the shape of a model. Besides, Hansen et al. [10] achieved a parallel printing process via microvascular multi-nozzle Arrays.

Multi-axis 3D printing

Song [24] and Pan et al. [20] developed a 6-DoF Steward mechanism to continuously print conformal features, such as textures or patterns, on curved and irregular surfaces. This CNC-based accumulative process enables continuous fabrication with different size, shape, and resolution requirements. Traditional multi-axis fabrication solutions might also reduce the need for support by tilting the nozzle or object. However, such systems have higher overhead such as a demanding control strategy for motion synchronization, complexity of mechanical calibration, and more importantly the difficulty of adhering print material onto largely slanted or bottom surfaces due to the effect of gravity. In our approach, by adding 1 DOF to a cuboid and using the printer's own X-, Y- and Z-step precision, we (a) add much greater functionality and capability to the resulting process and products, and (b) utilize gravity to allow the print material to firmly adhere to the rotated horizontal surfaces.

Printing with functional effect

There are also many research approaches dedicated to generate functional effects of fabricated products via geometric optimization on input models. Prevost et al. [21] proposed an approach to generate models which can stand alone by deforming the initial inputs. Umetani and Schmidt [26] optimized the orientation of a model for 3D printing to increase mechanical strength and structural soundness. Other interesting works involve printing kinematic mechanisms [1, 17], working prototypes [15], and articulated models [5, 3].

HOW REVOMAKER WORKS

In placing the cuboidal base within a desired shape, a key challenge is related to how to pose the objective function so the number of possibilities of cuboidal orientations and printing sequences are balanced to reduce the support generation as well as the use of print material. Furthermore, when printing one facet after the other, the print nozzle should not intersect with the material already printed, and merge the new partitioned shape well with the old. In this section, we first discuss how we formalize these objectives across many geometric shapes, followed by our mechanical implementation of RevoMaker.

Objective Function

Given an input triangular mesh model $M = (\mathcal{V}, \mathcal{E}, \mathcal{F})$, we introduce Cuboidization, an algorithm that generates an interior cuboid C, where all six facets C_f^i ($i \in (1, 2, ...6)$) of the cuboid partition M into six outward regions M_p^is. Recent research effort such as orthogonal slicing [11] and approximate pyramidal decomposition [13] introduce different partitioning strategies on the overall shape of an object to improve fabrication accuracy and for minimal number of pyramidal parts. In contrast, the main goals of our Cuboidization are two fold: (1) create the cuboid with as large volume as possible to save print materials, and (2) six outward regions M_p^i add up to as few overhangs as possible to save support material. Considering the time consumption and effort for post-processing, in our work the reduction of support material generation was given higher priority over augmenting the cuboid volume. Hence, we define the objective function as follows:

$$\arg\max_C F_{vol}(C) \quad s.t. \quad \sum_{i=1}^{6} F_{overhang}(M_p^i) = 0, \qquad (1)$$

where F_{vol} measures the volume of C and $F_{overhang}$ evaluates the overhanging feature of M_p^i. Evaluation of F_{vol} and $F_{overhang}$ is not a trivial task since $F_{overhang}$ depends on C but it can be only evaluated after the region partition is done. Therefore, it is not feasible to analytically solve Eq.1 using nonlinear optimization approaches.

In our work, an overhang-aware multi-loop optimization framework shown in Algorithm 1 is proposed to resolve this problem. The outer loop uses a *Particle Filtering* based sampling algorithm to generate a set of principal axes for the cuboid (also called *cuboidal orientation*), see Section "Initial orientation sampling". Inside the inner loop, by using three orthogonal vectors $\mathbf{u}$, $\mathbf{v}$ and $\mathbf{w}$ as the principal axes for the cuboid, we generate and compute the size of the largest cuboid inscribed (Section "Cuboid generation"). After obtaining the cuboids over all orientations, we compare their volume and overhanging features, and retain B top-ranked candidates with the least support consumption for the user to select the final print. How different printing sequences would affect the resultant partitioning as well as the avoidance of support generation is discussed in Section "Optimization of printing sequence". Currently, our Cuboidization algorithm is more suitable for processing shapes with topological genus

Algorithm 1: Multi-loop Cuboidization
***
Input: M is input model, l is the maximum level of Particle Filtering
Output: C is the cuboid that partitions M, and S is the printing sequence
Function $(C, S) = FindCuboidization(M, l)$
  | $currentLevel \leftarrow 0;$
  | $currentCuboidSet \leftarrow \varnothing;$
  | $newOrientationSet \leftarrow InitialOrientationSampling();$
  | **while** $currentLevel < l$ **do**
  | | **foreach** *orientation* $\mathbf{O}_i \in newOrientationSet$ **do**
  | | | $C \leftarrow GenerateCuboid(M, \mathbf{O}_i);$
  | | | $(C.V, C.A_{overhang}, C.S) = EvaluateCuboid(M, C);$
  | | | $currentCuboidSet \mathrel{+}= C;$
  | | $newOrientationSet = OrientationResampling();$
  | | $currentLevel \leftarrow currentLevel + 1;$
  | **return** $BestRanked(currentCuboidSet);$

Function $(V, A_{overhang}, S) = EvaluateCuboid(M, C)$
  | $V \leftarrow CalculateVolume(C);$
  | $A_{overhang} \leftarrow +\infty;$
  | **foreach** $S_{temp} \in All\ Printing\ Sequence\ for\ C$ **do**
  | | $A_{temp} \leftarrow CalculateOverhangingArea(M, C, S_{temp});$
  | | **if** $A_{temp} < A_{overhang}$ **then**
  | | | $A_{overhang} \leftarrow A_{temp};$
  | | | $S \leftarrow S_{temp};$
  | **return** $V, A_{overhang}, S;$
***

of 0, and preferably those that approximate the cuboid. Models with high genus (rings, knots, etc.), long and curved protruding features, or massive small curvy features, limit our approach towards providing less support structures.

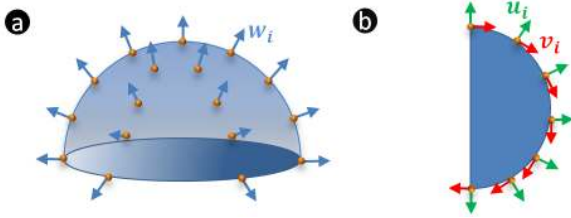**Overhang-aware Cuboidization framework**

Initial orientation sampling

Figure 4. (a) sampling the unit vector $\mathbf{w}_i$ (b) sampling the unit vectors $\mathbf{u}_i$ and $\mathbf{v}_i$.

In order to find an optimized interior cuboid for each model, we first consider sampling a set of cuboidal orientations using a particle filtering based approach. As each orientation matrix $\mathbf{O}_i$ consists of three unit orthogonal vectors $\mathbf{u}_i$, $\mathbf{v}_i$ and $\mathbf{w}_i$ as column vectors, the sampling is performed for the three components one after the other. Without loss of generality, $\mathbf{w}_i$ is determined initially. We uniformly sample K points on a Gauss sphere, and each of the samplings is assigned to $\mathbf{w}_i$ (see Fig.4 (a)). For each $\mathbf{w}_i$, the second uniform sampling is performed on a unit circle laying on the normal plane of $\mathbf{w}_i$ in order to obtain L samples of $\mathbf{u}_i$ and $\mathbf{v}_i$ (shown in Fig.4

(b)). Note that, as opposite direction results in the same $\mathbf{O}_i$, we consider herein only the semisphere and semicircle, where the polar point for semisphere and end point of semicircle are arbitrarily positioned. For each model, there are $K \times L$ orientations in total to be evaluated and filtered.

Cuboid generation

Given a determinate orientation, the second part of the algorithm generates a cuboid with as large volume as possible inside M. We use a heuristics-based method [6] to balance the resultant quality as well as computation efficiency. The generation details are as follows. Followed by the orientation $\mathbf{O}_i$, a small enough cuboid C_i is initialized at the center of a largest inscribed sphere within M. The six facets of C_i then move along their corresponding normal directions to incrementally expand the size of the cuboid. At each augmentation step, the corner collision is detected. The iteration stops when no facet can be moved further. All possible cuboids inscribed inside M along orientation $\mathbf{O}_i$ are recorded and indexed by volume, and the one with the maximum volume is returned as the resultant candidate .

Evaluation of overhangs

With the partitioned model, an overhanging evaluation function is defined as follows:

$$\sum_{j=1}^{6} \sum_{f_k \in \mathcal{F}_{M_p^j}} F_{area}(f_k), \tag{2}$$

$$F_{area}(f_k) = \begin{cases} 0 & if\ \mathbf{n}_{f_k} \cdot \mathbf{n}_{M_p^j} < \delta \\ area\ of\ f_k & otherwise \end{cases} \tag{3}$$

$F_{area}(f_k)$ measures the overhanging area on each facet f_k depending on whether the dot product of its normal $\mathbf{n}_{f_k}$ and the normal of C_f^j is less than the threshold. All results in this paper use δ to be $-\cos 45°$, unless otherwise stated.

Filtering and resampling

Based on the overhang evaluation, we select N orientations with the least sum of overhanging areas. To avoid selecting too many similar cuboids, we discard those orientations with less variation and only the ones with larger than 70% variations are kept. The following equation is used to evaluate the variation of two orientations $\mathbf{O}_i$ and $\mathbf{O}_j$:

$$\begin{aligned} F_{var} = &|\mathbf{u}_i \cdot \mathbf{u}_j| + |\mathbf{u}_i \cdot \mathbf{v}_j| + |\mathbf{u}_i \cdot \mathbf{w}_j| \\ &+ |\mathbf{v}_i \cdot \mathbf{u}_j| + |\mathbf{v}_i \cdot \mathbf{v}_j| + |\mathbf{v}_i \cdot \mathbf{w}_j| \\ &+ |\mathbf{w}_i \cdot \mathbf{u}_j| + |\mathbf{w}_i \cdot \mathbf{v}_j| + |\mathbf{w}_i \cdot \mathbf{w}_j| \end{aligned} \tag{4}$$

At each selected orientation, we uniformly resample over its neighborhood region with a radius ϵ on the Gauss sphere, and generate the new set of cuboids. The empirical values of K for initial sampling and resampling are set as 25 and 10. We use $L = 10$ for both samplings and $N = 5$ for the resampling process. Thus, for each model we evaluate 1250 orientations after two sampling processes in total. The final B top-ranked candidates with least support material generation are retained for user to select by leveraging the physical dimensions of functional components.
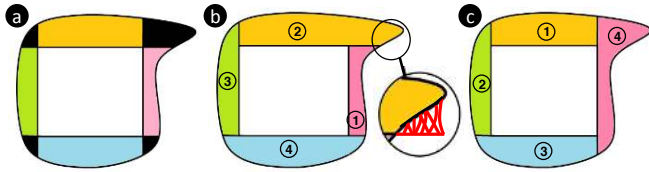
Figure 5. (a) partitioning based on above-facet regions and corner regions (b) printing sequence 1 generates support material (c) printing sequence 2 generates no support material.

Optimization of printing sequence

While evaluating the overhanging feature over six partitioned geometries, it is crucial to determine the optimal printing sequence simultaneously. In order to achieve the minimal number of rotations and therefore reduce the effort of handling, we define our strategy of printing such that: (1) four adjacent partitioned geometries about a central axis of the cuboid are printed by intermittently rotating about the axis by 90 degrees, and (2) the rest of the two opposite partitions are printed afterwards by rotating every 180 degrees about a second central axis which is orthogonal to the previous one. This reduces the number of degrees of freedom to two and the intermediate number of handling to one. Through initial partitioning, the model can be inherently segmented into the print regions right above each cuboidal facet (the pink, yellow, green and blue above-regions shown in Fig.5 (a)). As for the corner regions shown in black in Fig.5 (a), we assign each of them into its neighboring above-region(s). Here the printing strategy is that once the first facet is determined, each corner region is always assigned to the later-to-print above-region that follows a single rotational direction (for instance counterclockwise shown in Fig.5). In doing so, it also generates extended underlying surface to support the corner geometries after each rotation. Note that a different selection of the initial facet to be printed on results in different support generation scenarios. As shown in Fig.5, the sequence (b) requires support in the right upper corner while in (c) it is totally support-free hence the better choice. For each cuboid with determinate size and orientation, we search over 30 different combinations of printing sequence around six cuboidal facets and choose the one with less or no support generation. These combinations vary based on which facet is the first to
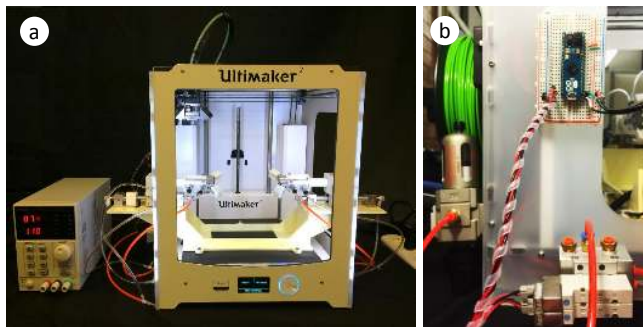
be printed on, the rotational direction and the selection of two facets that stay as the last-to-print ones.

Mechanical implementation behind RevoMaker

Ultimaker 2 Printer

Our machine design goal is to enhance an existing 3D printer at minimal cost and augmented complexity. Fig.6 (a) shows an assembled view of the mechanical and electrical apparatus that are extended onto Ultimaker2. All of the models shown in this paper were printed on this modified 3D printer, i.e., an open-source fused-filament extrusion system with $230mm \times 225mm \times 205mm$ build volume and up to 20 microns print accuracy. The filament material used for printing is the $3mm$-diameter Polylactic acid (PLA).

Laser cutting a cuboidal base

Unlike the standard bed material used in FDM printers where extruded plastic needs to be easily peeled off from the print bed, we select a $3mm$-thick *Plexiglas*® DP-95 acrylic sheet as the build surface material for each facet of the cuboidal base. This cell-cast material is available with low heat capacity and matte finish on both sides to ensure a very firm first-layer PLA bonding without any pre-heating process.
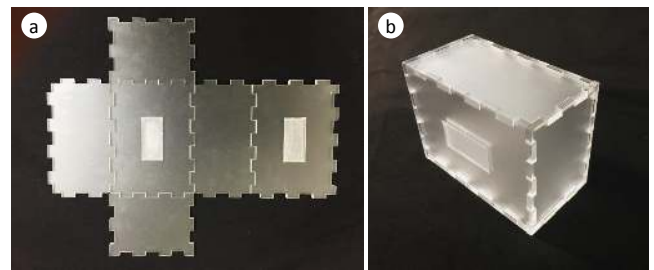

Figure 7. (a) a flattened cuboidal net pattern using laser-cut facets and slots; (b) a folded cuboid.

Six rectangular facets and twelve edges comprise a cuboidal base. We synthesize the interlocking teeth pattern along each edge so that six facets can be rapidly press-fit together seamlessly (see Fig.7). In order to level and secure the cuboid during printing, two $32mm \times 15mm$ rectangular slots are also engraved on a pair of opposite cuboidal facets (also called side-facets) using laser cutting. Our experimental results show that for each model it takes on the average 5 to 10 minutes to laser cut the facets and approximately 1 minute to assemble the cuboid.

Embedding of functional modules

The internal space inside each cuboid base is utilized for embedding functionalities. This standardized cuboidal space can house a wide variety of mechanical, electronic, sensory and actuation components, including but not restricted to processor chips, sensors, springs, gears and motors. By providing channels in the printed material, external devices such as lights and wind-up keys can then interconnect with the housed components inside to enhance visual, motion and movement functionalities, through the slots and holes already added on each of six cuboidal facets. Our process is relatively simple when compared to the traditional processes

Figure 6. We extend a standard low-cost FDM printer, UltiMaker 2, with mechanical, electrical and pneumatic devices.
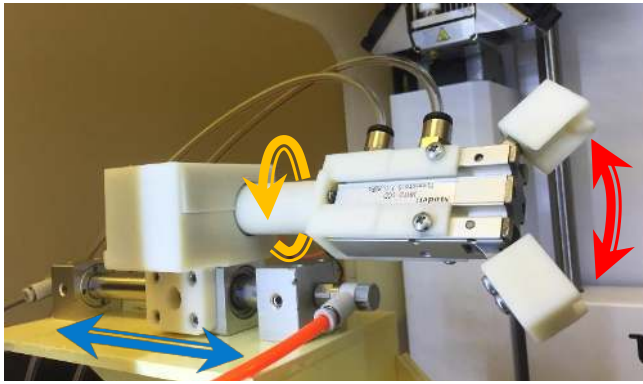
Figure 8. Each gripper from both sides has 3 degrees-of-freedom: (1) translation to fixate and release the cuboidal base, (2) rotation to revolve the cuboid facets around, and 3) angular motion to apply gripping force to the handles.

where multiple high-fidelity printed parts must be assembled in 3D while enclosing motors and sensors. We lay down and pre-assemble functional modules on the "flat" unfolded cuboid. We then close the cuboid by folding, and "coat" the external skin shapes over it using our 3D printing process.

Fixation, revolving and gripping
Three degrees-of-freedom are needed for realizing the multi-directional printing: (1) translation along X to fixate and release the cuboidal base, (2) rotation about X to revolve the cuboid facets around, (3) and angular motion to deliver strong gripping to the handles. We attach an acrylic stand with 2 cantilevered support plates to our build platform. A pair of linear air cylinders sits on the support plates to fixate or release the cuboid from both sides. These magnetically coupled linear cylinders (CY3R-10-65) are powered pneumatically and controlled by a solenoid valve (see Fig.6 (b)). To enable the rotation, two HerkuleX DRS-0201 robot servos rest on the air cylinders and two connected air fingers (MHY2-10D) provide angular gripping motion. In RevoMaker, we first hand deliver the cuboidal base to the center of the printer. These 180-degree air fingers are initially closed and fit into side slots to secure the cuboid by squeezing. After one partitioned geometry is printed on top of the build surface, the servos synchronously rotate the base by 90 degrees. Therefore, four facets surrounding the revolute axis can be printed in the first run of rotation (see Fig.9 (b)-(e)). Note that during printing, two opposite facets among the four are chosen to add two collinearly-aligned handles outside the geometries. The purpose of adding these handles is for the grippers to secure the model in the second run of rotation while avoiding directly contact with the printed surface .

After we releasing the grippers, we rotate the part such that the grippers close over the handles from both sides. Once the remaining two partitioned geometries are printed, we snap off two handles for completing the print. Throughout the whole fabrication process, we calibrate the surface location of the cuboid twice before printing the first and the fifth facets. The corner coordinates of the rectangular facets and slots are recorded as the reference coordinates for the print head to start printing.

ALGORITHMIC AND PROTOTYPICAL RESULTS

Sculptural objects
According to the Cuboidization results on a number of genus 0 models with different overhanging features on different locations, including man-made art objects and organic forms, our optimization framework generates cuboids that allow zero support material to the printed geometries. Five sculptural models including a small Hexacronic Icositetrahedron, spherical ball, Max Planck, French bulldog, and Mickey Mouse were fabricated to verify our optimization framework with reduction of print and support material. Fig.9 (a) shows the partitioned result of a small Hexacronic Icositetrahedron where 6 "mountain"s are extruded and connected from 6 cuboidal facets, respectively. After laser cutting the cuboid and print-
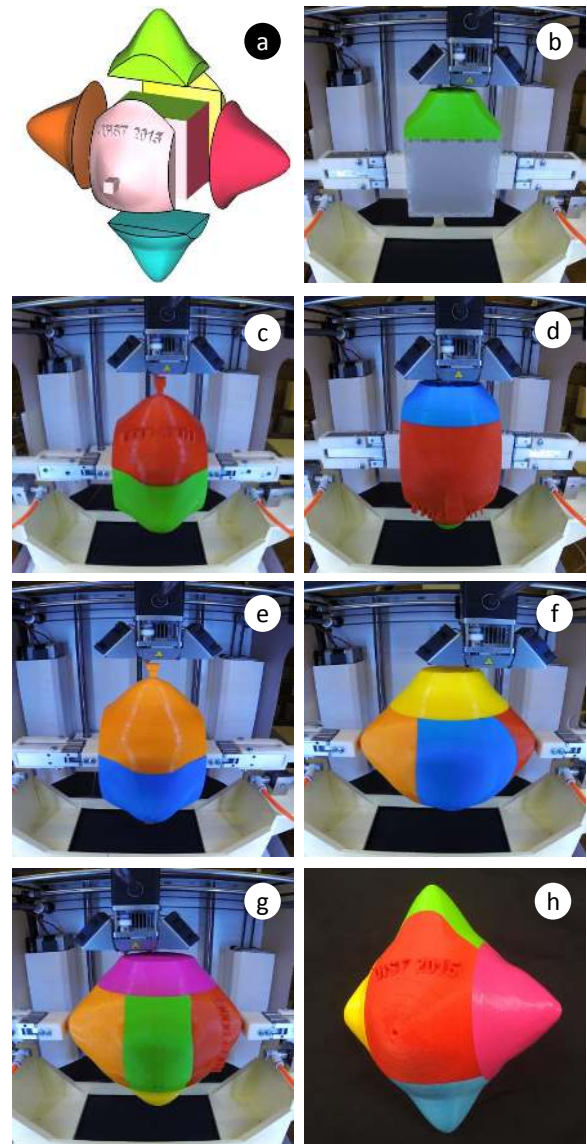

Figure 9. (a) Cuboidal generation and partitioned results of a small Hexacronic Icositetrahedron with the "UIST 2015" logo. (b)-(g) printing 6 partitioned geometries intermittently around a revolving cuboidal base using our method. (h) final print.

Table 1. Comparison of time and total material reduction using RevoMaker and Ultimaker 2.

Models	RevoMaker		Ultimaker 2				time reduction	total material reduction
	total time (hh:mm)	build volume (cm^3)	time (hh:mm)		build volume (cm^3)			
			t_{min}	t_{max}	V_{min} ($V_{support}$)	V_{max} ($V_{support}$)	compared to t_{min}	compared to V_{min}
Sphere	**4:03**	**61.7**	4:58	4:58	77.9 (0.3)	77.9 (0.3)	18.4%	20.8%
Max Planck	**6:11**	**114.6**	8:13	9:16	142.6 (7.4)	163.8 (28.6)	23.5%	19.6%
Bulldog	**7:36**	**133.8**	10:52	12:43	177.3 (26.7)	215.9 (65.3)	20.8%	24.5%
Mickey	**6:15**	**112.2**	8:22	15:01	138.4 (6.4)	257.2 (125.2)	25.3%	18.9%
Star	**9:06**	**165.5**	11:25	13:32	200.6 (12.6)	231.9 (43.9)	20.3%	17.5%
PC Mouse	**2:55**	**48.4**	4:38	6:44	76.7 (10.9)	111.3 (45.6)	37.0%	36.8%
Bulbasaur	**5:24**	**93.7**	6:37	7:17	109.7 (1.7)	121.6 (13.6)	18.39%	14.6%

*By placing a model in different orientations, t_{min} and t_{max} are the minimum and maximum time duration using Ultimaker 2; V_{min} and V_{max} are the minimum and maximum consumption of overall material (build + support), $V_{support}$ is only the consumption of support material. Using RevoMaker, the time statistics of Cuboidization for each selected model (top down), included in the total time, are 30s, 2min 33s, 6min 45s, 5min 03s, 1min 10s, 1min 02 s, 4 min 17s, respectively.

ing around each facet (see Fig.9 (b)-(g)), we achieve the final print with 6 different colors and a "UIST 2015" logo on it. Fig.10 shows the rest of the models with their support generation using Ultimaker 2, partitioned results and final prints using RevoMaker. In order to validate the strength in our approach to save time, build material and support material, we compare the fast-printing results using both RevoMaker and Ultimaker 2 over seven selected models.
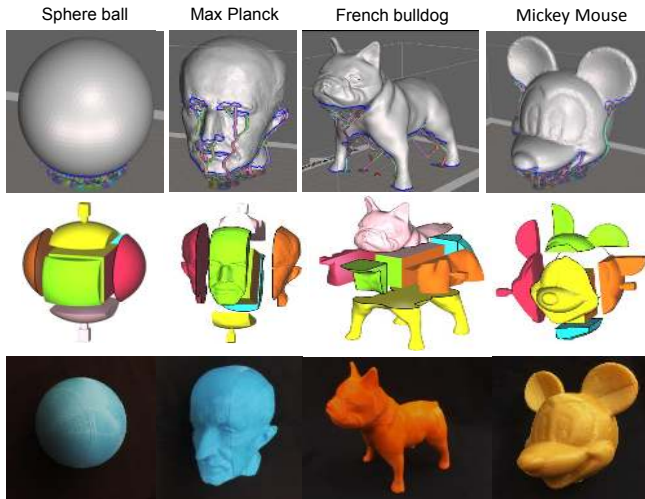

Figure 10. first row: visualization of support generation for a sphere ball, Max Planck, French bulldog and Mickey Mouse head using existing FDM printing process in Ultimaker2 (the model is oriented where less support structures are created. second row: partitioned results of each model. third row: prototypical results of each model

As shown in Table. 1, comparing to t_{min} and V_{min}, Revomaker achieves a 23.4% reduction of printing time, and 21.8% reduction of total material consumption on average using the lightest infill setup. The main strength of our multi-directional printing process is that it provides significant reduction of support material generation. We observe that the regular unidirectional extrusion process initially generates skirts and rafts on the print bed to smooth the printing flow and to assist bed adhesion, then it prints 3~4 solid adhering layers and followed by the hollowed structures inside. Our approach requires periodically printing 1 adhering layer 6 times for the six partitioned geometries. Together with the

two added handles, it leads to a modest improvement in printing time and overall material consumption.

Custo "mice": Customizable mice

We customize a computer mouse for an ergonomical fit to the palm and tailored functionalities. Dating back to 1964, Dr. Douglas Engelbart invented the first computer pointing device with one button on top and two wheels on the underside. The mouse began to multiply rapidly with embedded mechanical, optical and electronic systems. However, creating a mouse design from scratch and prototyping enclosures can be an iterative and daunting task especially for novices. It requires 3D modeling, molding/tooling design and physical assembly to be integrated seamlessly to fit all individual components inside an exterior shell. In addition, with traditional injection molding, it is difficult to mold reentrant features and side-surface functions such as buttons.
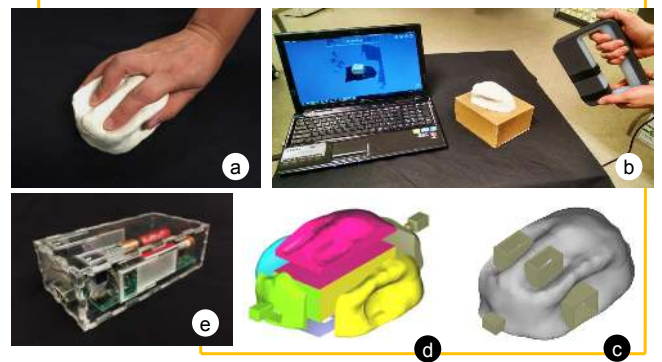

Figure 11. shows (a) user interaction to tailor the shape of his/her ergonomical-fitting mouse using Play Doh, (b) 3D scanning, (c) hollowing the digital model with slot-cuts to separate out three button areas, (d) six partitioning geometries around an embedded cuboid, and (e) enclose buttons, printed circuit board and optical components inside the laser-cut cuboid.

To demonstrate the whole fabrication process, Play Doh was initially used to create the shape of the mouse (see Fig.11 (a)). In doing so, the user is able to quickly verify a list of customizable human factors regarding the size range of hands, finger extension and palm comfort. In our custo"mice" the user also specifies the middle-click to be operated by thumb
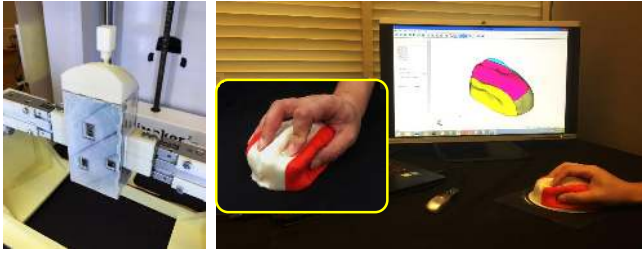
Figure 12. Revomaker prints the partitioned geometries around the cuboidal enclosure and delivers a functional and ergonomical computer mouse right after printing.

on the side of the mouse. Then its shape was captured using a 3D scanner, shown in Fig.11 (b). The algorithm generates the size of the cuboidal base and provides slot-cuts for the button areas in the partitioned geometries, shown in Fig.11 (c,d). Matching slot-cuts on the cuboid provide a cantilever which deflects to actuate internal switch when the external button area is pressed. Fig.11 (e) shows that all added functional modules are pre-assembled on the flattened laser-cut facets and enclosed inside the cuboid when closed. These modules include 3 buttons for left-, middle-, and right-clicking; light-emitting diodes (LEDs) and photodiodes to detect movement relative to the underlying surface; printed circuit board (PCB) with electrical resistors, capacitors, integrated circuits (ICs) mounted on; and rechargeable battery. Lastly, the custom-made geometries are printed around the cuboid to complete

the prototyping and ready for use directly after printing (see Fig.12).

Wind-up Pokémon

To further expand the design space for functional products, we enclose passive-actuated wind-up motor with gears and springs inside the cuboidal base. One of the popular Pokémon characters, Bulbasaur, was selected in this example due to its large amount of overhanging features, shown in Fig.13 (a). Similar to the previous procedures, we partition six geometries around an embedded cuboid (see Fig.13 (b)), and enclose the cuboid with laser-cut facets and kinematic components including the wind-up motor and batteries (see Fig.13 (c)). After taking it out from Revomaker, we insert another Pokémon character Pikachu's tail into the back hole of Bulbasaur, and a wind-up key into the side hole of Bulbasaur to waggle the tail. Besides, one can insert a pair of LEDs into the eyes of Bulbasaur, and the eyes start blinking simultaneously after winding, shown in Fig.13 (e).

CONCLUSION AND FUTURE WORK

In this paper, we have explored a multi-directional 3D printing process to not only reduce the consumption of print and support material, but also to enable a new breed of custom products with embedded functionalities. We propose the Cuboidization algorithm to generate a cuboidal enclosure, that is also the printing base. It has as large a volume inside the model and with as few overhangs as possible. Using Revomaker, we printed a number of sculptural models and two functional products, i.e., a customizable computer mouse and wind-up toy. We thus demonstrated its capabilities in combining functional design along with the shape creation.

Figure 14. shows inapplicable cases where overhanging features can not be largely reduced. For instance, (a) a 3D shape with high topological genus such as a ring of genus one, or (b) with long and branched protruding features such as a tree.
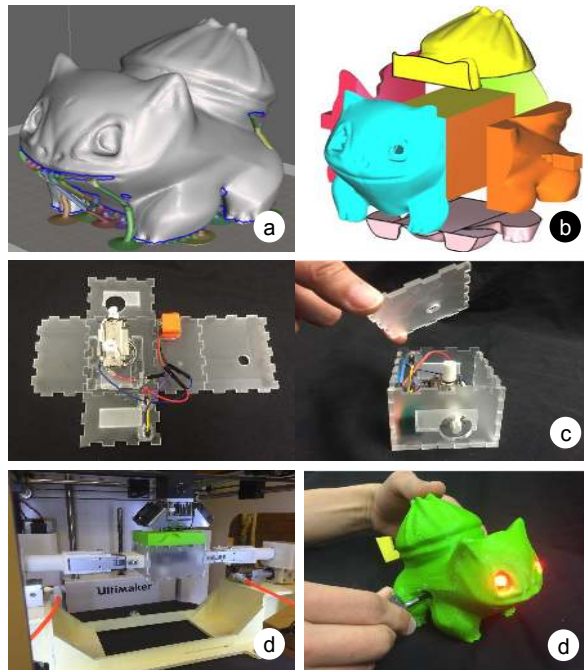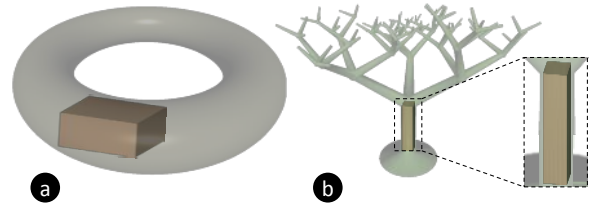

Figure 13. shows (a) support generation for Bulbasaur, (b) six partitioning geometries around an embedded cuboid, (c) pre-assembling the wind-up motor and batteries onto flattened laser-cut facets and closing the cuboid as a printing base, (d) printing the Bulbasaur shape around the cuboid, and (e) winding the Bulbasaur up to trigger tail-waggling and eye-blinking.

As future work, we will explore the extension of our current Cuboidization algorithm to generate a prismatic polyhedral structure as the printing base, in order to further reduce the support consumption. In doing so, the overhanging features on a model can be further partitioned and eliminated while printing over more polyhedral facets. In addition, for complex geometries that cannot be approximated by a single cuboid, we will explore using sub-cuboids for better approximation, and to further minimize the print and support generation. This also allows additional functions to be encapsulated inside multiple enclosures. For those 3D shapes with high genus, long protruding and massive curvy features, our approach still requires support generation after partitioning, see in Fig.14. We believe that the modularization of functionalities and integration of 3D shapes will open up a new genre

of 3D printing and eventually alleviate design and assembly burdens.

ACKNOWLEDGMENTS

REFERENCES FORMAT

References must be the same font size as other body text.

REFERENCES

1. Alam, M., Mavroidis, C., Langrana, N., and Bidaud, P. Mechanism design using rapid prototyping. In *Proceedings of the 10th World Congress on the Theory of Machines and Mechanisms* (1999), 930–938.

2. Alexander, P., Allen, S., and Dutta, D. Part orientation and build cost determination in layered manufacturing. *Computer-Aided Design 30*, 5 (1998), 343 – 356.

3. Bächer, M., Bickel, B., James, D., and Pfister, H. Fabricating articulated characters from skinned meshes. *ACM Trans. Graph. 31*, 4 (July 2012), 47:1–47:9.

4. Beyer, D., Gurevich, S., Mueller, S., Chen, H., and Baudisch, P. Platener: Low-fidelity fabrication of 3d objects by substituting 3d print with laser-cut plates.

5. Calì, J., Calian, D., Amati, C., Kleinberger, R., Steed, A., Kautz, J., and Weyrich, T. 3d-printing of non-assembly, articulated models. *ACM Trans. Graph. 31*, 6 (Nov. 2012), 130:1–130:8.

6. Chebrolu, U., Kumar, P., and Mitchell, J. On finding large empty convex bodies in 3d scenes of polygonal models. In *Computational Sciences and Its Applications, 2008. ICCSA '08. International Conference on* (June 2008), 382–393.

7. Crump, S. Apparatus and method for creating three-dimensional objects, Jun 1992. US Patent 5,121,329.

8. Deckard, C. Method and apparatus for producing parts by selective sintering, Sep 1989. US Patent 4,863,538.

9. Dumas, J., Jean, H., and Sylvain, L. Bridging the gap: automated steady scaffoldings for 3d printing. *ACM Transactions on Graphics (TOG) 33*, 4 (2014), 98.

10. Hansen, C., Saksena, R., Kolesky, D., Vericella, J., Kranz, S., Muldowney, G., Christensen, K., and Lewis, J. High-throughput printing via microvascular multinozzle arrays. *Advanced Materials 25*, 1 (2013), 96–102.

11. Hildebrand, K., Bickel, B., and Alexa, M. Orthogonal slicing for additive manufacturing. *Computers & Graphics 37*, 6 (2013), 669–675.

12. Hu, K., Jin, S., and Wang, C. C. Support slimming for single material based additive manufacturing. *Computer-Aided Design 65*, 0 (2015), 1 – 10.

13. Hu, R., Li, H., Zhang, H., and Cohen-Or, D. Approximate pyramidal shape decomposition. *ACM Transactions on Graphics (TOG) 33*, 6 (2014), 213.

14. Hull, C. Apparatus for production of three-dimensional objects by stereolithography, Mar 1986. US Patent 4,575,330.

15. Koo, B., Li, W., Yao, J., Agrawala, M., and Mitra, N. Creating works-like prototypes of mechanical objects. *ACM Transactions on Graphics (TOG) 33*, 6 (2014), 217.

16. Lu, L., Sharf, A., Zhao, H., Wei, Y., Fan, Q., Chen, X., Savoye, Y., Tu, C., Cohen-Or, D., and Chen, B. Build-to-last: Strength to weight 3d printed objects. *ACM Trans. Graph. 33*, 4 (July 2014), 97:1–97:10.

17. Mavroidis, C., DeLaurentis, K., Won, J., and Alam, M. Fabrication of non-assembly mechanisms and robotic systems using rapid prototyping. *Journal of Mechanical Design 123*, 4 (2001), 516–524.

18. Mueller, S., Im, S., Gurevich, S., Teibrich, A., Pfisterer, L., Guimbretière, F., and Baudisch, P. Wireprint: 3d printed previews for fast prototyping. In *Proceedings of the 27th Annual ACM Symposium on User Interface Software and Technology*, UIST '14, ACM (New York, NY, USA, 2014), 273–280.

19. Mueller, S., Mohr, T., Guenther, K., Frohnhofen, J., and Baudisch, P. fabrickation: Fast 3d printing of functional objects by integrating construction kit building blocks. In *CHI '14 Extended Abstracts on Human Factors in Computing Systems*, ACM (New York, NY, USA, 2014), 187–188.

20. Pan, Y., Zhou, C., Chen, Y., and Partanen, J. Fabrication of conformal ultrasound transducer arrays and horns based on multi-axis cnc accumulation. In *ASME 2011 International Manufacturing Science and Engineering Conference*, American Society of Mechanical Engineers (2011), 39–48.

21. Prévost, R., Whiting, E., Lefebvre, S., and Sorkine-Hornung, O. Make it stand: Balancing shapes for 3d fabrication. *ACM Trans. Graph. 32*, 4 (July 2013), 81:1–81:10.

22. Sachs, E., Haggerty, J., Cima, M., and Williams, P. Three-dimensional printing techniques, Apr 1993. US Patent 5,204,055.

23. Schmidt, R., and Umetani, N. Branching support structures for 3d printing. In *ACM SIGGRAPH 2014 Studio*, SIGGRAPH '14, ACM (New York, NY, USA, 2014), 9:1–9:1.

24. Song, X., Pan, Y., and Chen, Y. Development of a low-cost parallel kinematic machine for multidirectional additive manufacturing. *Journal of Manufacturing Science and Engineering 137*, 2 (2015), 021005.

25. Thrimurthulu, K., Pandey, P., and Reddy, N. Optimum part deposition orientation in fused deposition modeling. *International Journal of Machine Tools and Manufacture 44*, 6 (2004), 585 – 594.

26. Umetani, N., and Schmidt, R. Cross-sectional structural analysis for 3d printing optimization. *SIGGRAPH Asia* (2013), 5.

27. Vanek, J., Galicia, J., and Benes, B. Clever support: Efficient support structure generation for digital fabrication. *Computer Graphics Forum 33*, 5 (2014), 117–125.

28. Wang, W., Wang, T., Yang, Z., Liu, L., Tong, X., Tong, W., Deng, J., Chen, F., and Liu, X. Cost-effective printing of 3d objects with skin-frame structures. *ACM Trans. Graph. 32*, 6 (Nov. 2013), 177:1–177:10.